Journal of Animal & Plant Sciences, 35(2): 2025, Page: 429-444
ISSN (print): 1018-7081; ISSN (online): 2309-8694
https://doi.org/10.36899/JAPS.2025.2.0036

EVALUATING ADSORPTION KINETICS OF ENDOSULFAN ON NATURAL AND SYNTHETIC ADSORBENTS: A COMPARATIVE STUDY

M. A. Hussain[1], G. Murtaza[1*], M. Zia-ur-Rehman[1], M. Shahid[2] and S. Calero[3]

[1]Institute of Soil and Environmental Sciences, University of Agriculture, Faisalabad, 38040-Pakistan
[2]Department of Biochemistry, University of Agriculture, Faisalabad, 38040-Pakistan
[3]Department of Applied Physics, Eindhoven University of Technology, Eindhoven, Netherlands
[*]Corresponding author's Email: gmurtaza@uaf.edu.pk; gmurtazauaf@gmail.com

ABSTRACT

The present study investigates the adsorption of endosulfan from aqueous solutions using various low-cost adsorbents. Adsorption kinetic data were analyzed using different models to determine the most effective adsorbents. In this study, different adsorbents, including sawdust, sugarcane bagasse, corncob, sawdust biochar, sugarcane bagasse biochar, corn-cob biochar, zeolite, montmorillonite, kaolinite, and magnetite, were applied at a rate of 0.02 g L^{-1}. Endosulfan was spiked at concentrations of 0.01, 0.05, 0.1, 0.5, and 1 mg L^{-1}. For kinetic studies, samples were collected at different time intervals (1, 3, 5, 8, 16, and 24 hours). The results revealed that natural zeolites exhibited the highest removal efficiency among all tested materials, with maximum adsorption capacity between 8 and 16 hours. Due to their large surface area, interlayer ions, and surface charge, clay minerals demonstrated a superior adsorption capacity compared to other adsorbents. Among the kinetic models, the pseudo-second-order model best described the adsorption behavior of most adsorbents, except for montmorillonite. Based on the intra-particle diffusion model, K_{id} values for sawdust, corncob biochar, and montmorillonite were 0.3093, 0.3075, and 0.3067 (mg g^{-1} $s^{-0.5}$), respectively. For montmorillonite, the Qe Exp was 1.89 mg g^{-1}, while Qe max predicted by pseudo-first-order and second-order models were 1.93 and 2.02 mg g^{-1}, respectively. The pseudo-first-order model showed a better fit (R^2 = 0.977, and R^2 = 0.99) confirming the correlation. It is concluded that natural zeolites are the most effective adsorbent for endosulfan removal, with the pseudo-second-order model best describing adsorption kinetics for most materials.

Key words: Endosulfan; Low-cost adsorbents; Clay minerals; Zeolites; Montmorillonite; Biochar; Chemisorption.

Published first online February 22, 2025 Published final April 28, 2025

INTRODUCTION

Pesticides are crucial in modern agricultural practices, contributing to increased crop yields and pest management. However, their widespread use has raised serious environmental and health concerns, where pesticide residues have been reported to contaminate soil and groundwater (Abbas *et al*., 2024). Among these pesticides, endosulfan, a widely used organochlorine insecticide, has been recognized for its effectiveness and low cost. However, its bioaccumulative nature, environmental persistence, and acute toxicity pose significant risks to ecosystems and human health (Bhanot and Pant, 2025). Endosulfan is a synthetic compound primarily used for pest suppression (Jacobson, 2021). Its toxic effects include organ damage, seizures, and, in severe cases, respiratory failure leading to death (Dilna *et al*., 2018; Liu *et al*., 2017). Exposure through ingestion, inhalation, or dermal absorption has been linked to neurological disorders, reproductive defects, and carcinogenic potential (Fantke and Jolliet, 2016; Li and Jennings, 2017).

Several remediation techniques, including chemical, physical, and biological methods, have been explored for pesticide decontamination (Saleh *et al*., 2020). Solid biowastes (biosorbents) derived from the food industry and agricultural residues have gained attention due to their cost-effectiveness and environmental sustainability (Ashraf *et al*., 2017). Biosorption presents multiple advantages over conventional methods, such as ease of operation, high removal efficiency, minimal waste production, and potential resource recovery (Shakoor *et al*., 2016). Various materials, including wood charcoal (Liu *et al*., 2024), low-cost natural organic substances (Aziz *et al*., 2024), aerobic mixed bacterial cultures (Martínez-Burgos *et al*., 2024), and wheat straw (Aslan and Türkman, 2004), have been explored for endosulfan removal. While these approaches have shown promising results, they often suffer from limitations such as incomplete degradation, secondary pollution, and high operational

costs, highlighting the need for more efficient and sustainable alternatives.

Clay minerals, particularly bentonite, have been extensively studied for adsorption capabilities due to their large surface area, high cation exchange capacity, and strong affinity for organic and inorganic contaminants (Durán *et al*., 2019; Obsa *et al*., 2024). Bentonite has been found effective in removing various pollutants, including malathion, UO_2^+ ions (Karami-Mohajeri and Abdollahi, 2011), and heavy metals such as Cd and Pb under estuarine and seawater conditions (Karim *et al*., 2019). Natural and activated bentonite has also demonstrated the ability to adsorb Cd and Zn at 30ºC (Tahervand and Jalali, 2017). Similarly, other clay minerals like kaolinite and montmorillonite have been employed for wastewater remediation and heavy metal adsorption due to their electrostatic interactions and complexation abilities (Fraiha *et al*., 2024; Mokhtar *et al*., 2024). Clay minerals have a high swelling capacity and surface area, making them effective in absorbing heavy metals (Wang *et al*., 2024; Khandamov *et al*., 2025). Metal removal occurs through ion exchange, where its negatively charged surface attracts metal cations like Pb, Cd, and Ni. They also adsorb metals via electrostatic interactions and can form complexes through surface functional groups, further immobilizing the metals (Bulgariu *et al*., 2024). Kaolinite removes heavy metals through surface adsorption, attracting metal ions like Cr and Zn via electrostatic forces and hydrogen bonding (Li *et al*., 2025; Sam *et al*., 2025). It also exchanges metal ions with other cations in the soil and may promote the precipitation of metal hydroxides, further removing metals (Sam *et al*., 2025). Montmorillonite removes heavy metals through high cation exchange capacity, adsorbing ions like Cd, Pb, and Cu on its surface. Its layered structure traps metals between the layers, and complexation reduces their mobility and bioavailability (Zhao *et al*., 2024).

Agricultural wastes such as sawdust, sugarcane bagasse, corncobs, and wheat straw are abundant and inexpensive materials that can be used directly or modified to enhance their adsorption properties (Liu *et al*., 2022; Mubarak *et al*., 2024). These wastes contain cellulose, hemicellulose, and lignin, which have hydroxyl, carboxyl, and other reactive groups that interact with pesticide molecules through hydrogen bonding, van der Waals forces, and electrostatic interactions (Juela, 2022; Khoo *et al*., 2018). Agricultural residues have a high organic carbon content that can enhance the sorption of hydrophobic pesticides like endosulfan, reducing their mobility and bioavailability in the environment (Zhou and Wang, 2020). The pyrolysis of agricultural waste into biochar significantly increases its surface area and pore structure, improving pesticide retention through physical and chemical adsorption (Mandal *et al*., 2017). Biochar contains various functional groups (e.g., hydroxyl, carboxyl, and aromatic rings) that enhance its interaction with organic contaminants, including pesticides (Liu *et al*., 2018). The surface charge and cation exchange capacity of biochar influence pesticide adsorption, particularly for ionizable pesticides, improving contaminant immobilization (Ogura *et al*., 2021). Most previous research has focused on individual adsorbents (e.g., clays, biochar, or natural organic materials) rather than a comparative assessment of multiple low-cost materials. The relative performance of biochar, clays, and agricultural waste in removing endosulfan under similar environmental conditions remains poorly understood. It was hypothesized that low-cost natural and synthetic adsorbents can effectively remove endosulfan from contaminated water, with adsorption kinetics governed primarily by the pseudo-second-order model, influenced by factors such as adsorbent type and contact time. The main objectives of this study were: 1) to quantify the removal efficiency of endosulfan from wastewater using various novel organic and inorganic solid-phase adsorbents under different experimental conditions; 2) to evaluate the adsorption mechanisms by applying kinetic models and distinguishing between chemisorption and physisorption processes; 3) to identify the optimal adsorbent concentration for maximizing endosulfan adsorption in aqueous systems.

MATERIALS AND METHODS

Adsorbents preparation: Endosulfan, NaOH (~97% pure), HCl, and ethanol (95%) were sourced from Sigma Chemical and purchased from UH Analytical Supplies of Faisalabad, Pakistan; all chemicals were analytical grades. Three clay minerals (zeolite, kaolinite, montmorillonite) and feedstocks (sawdust, sugarcane bagasse, corncob), along with their biochars and magnetite (iron oxide), were used for adsorption studies.

Sugarcane bagasse and corncob were collected from the Directorate of Farms, UAF. Saw dust was collected from a furniture market, in Sadar Bazar, Ghulam Muhammad Abad, Faisalabad. All collected samples were dried in an oven at 65 °C for 48 h. To achieve a homogeneous size, adsorbents were perched in a mechanical grinder. Biochars were produced through pyrolysis at 500°C in a muffle furnace at the University of Agriculture, Faisalabad, under oxygen-free conditions. Sugarcane bagasse, corncobs, and sawdust were first oven-dried, finely ground, and placed in the furnace chamber for thermal decomposition. The controlled heating converted the organic materials into biochar by removing volatile compounds and enhancing carbon stability. After pyrolysis, the biochar was cooled within the furnace, sieved for uniformity, and stored in airtight jars to preserve its adsorption properties for experimentation.

Magnetite and zeolite, with 99% purity and particle sizes of 100 and 150 mesh, respectively, were obtained from Gongyi City Meiqi Co., Ltd., Henan, China. Kaolinite and montmorillonite (99% pure) were obtained from Guangzhou Billion Peak Chemical Technology Co. Ltd., Guangdong, China. Feedstock and their biochars were kept at ambient temperature (25-27 °C) for seven days in the laboratory and then oven-dried for three days at 65°C prior to crushing in an electric mixer. The sieving of crushed feedstock and their biochars was carried out by using a vibrating sieving machine, and the final product, having a particle size < 250 mesh, was stored in airtight jars.

Characterization of adsorbents: The surface morphologies of natural adsorbents and their biochars obtained via different pyrolysis temperatures as well as clay minerals and magnetite were characterized through a scanning electron microscope (SEM). Attenuated total reflectance-Fourier transform infrared spectroscopy (ATR-FTIR) spectra were used for the identification of surface functional groups. For this, a small amount of powdered adsorbent was mixed with powdered potassium bromide (KBr), pressed into a pellet, and placed into a pellet holder for instrumental analysis. X-ray diffraction (XRD) was used for the basic characterization of the low-cost adsorbents.

Experimentation: High purity (99.1%) endosulfan was taken to prepare a stock solution using 1% methanol (95% purity; Sigma). All the glassware was initially acid washed using 5% nitric acid (HNO_3; BDH, Germany) and then washed twice with distilled water before use. The stock solution was kept in an amber glass bottle to avoid any degradation through UV radiation.

Batch experiment: A batch adsorption experiment was carried out at room temperature (25 ± 2 °C). An endosulfan stock solution (1000 mg L^{-1}) was initially prepared in 1% methanol, and a series of dilutions using double deionized water were prepared to obtain the desired range of endosulfan concentration. Batch adsorption experiments were performed in 100 mL beakers containing endosulfan solution (50 mL) of different concentrations (0.01, 0.05, 0.1, 0.5, and 1 mg L^{-1}) and a fixed adsorbent dose (0.02 g). The combined solution was stirred using a reciprocating shaker (100 rpm) at ambient temperature. For kinetic studies, samples were collected at varying time intervals (1, 3, 5, 8, 16, and 24 h), followed by filtration, and the residual endosulfan concentration in solution was measured using a UV-visible spectrophotometer at 310 nm from the solution phase. A series of batch adsorption experiments were carried out to evaluate the adsorption potential of all the adsorbents selected, including adsorption (1) kinetics, (2) isotherm, and (3) edges.

Data analysis

Adsorption Kinetics: Kinetic studies were conducted with various adsorbents using pseudo-first-order, pseudo-second-order, and intra-particle diffusion models. In the second-order model, surface-active sites limit the rate. Removal from solution is due to physicochemical interactions between solid functional groups and aqueous chemicals (Singh *et al*., 2018). The pseudo-first-order model is given by Eq. (1).

$$\frac{dq_t}{dt} = K_1 (q_e - q_t) \qquad (1)$$

Where, $\frac{dq_t}{dt}$ is the rate of change of adsorbed substance over time. K_1 is the first-order rate constant. qe is the equilibrium adsorption capacity. qt is the adsorption capacity at time t.

$$\text{Log } (q - q) = \log q - \frac{k_1}{2.303} t \qquad (2)$$

$$\frac{dq_t}{dt} = K_2 (q_e - q_t)^2 \qquad (3)$$

$$\frac{t}{(q_t)} = \frac{1}{k_2 q_e^2} + \frac{1}{q_e} t \qquad (4)$$

The intra-particle diffusion model describes mass transfer in an amorphous sphere (Cooney *et al.,* 1999), with diffusion stages identified by linearizing curve portions (Wu *et al*., 2001).

$$q_t = f / (t^{1/2}) \qquad (5)$$

where, *qt* is the amount of adsorbate adsorbed at time t. f is the intra-particle diffusion rate constant for adsorption. t is time.

Adsorption isotherm: Adsorption isotherm equilibrium was performed by using different concentrations of Endosulfan (0.01, 0.05, 0.1, 0.5, and 1 mg L^{-1}) by using an adsorbent dose (0.02 g), incubated in the orbital shaker, stirring at the rate of 200 rpm at room temperature for 24 h. After 24 h, the remaining concentration of endosulfan was measured by using a spectrophotometer from each of the solutions. From every solution, the sample was collected with the help of a polypropylene syringe (0.2 µm) filter to determine the bioavailable concentration of endosulfan calculated by difference Eq. (6).

$$Q = \frac{(Ci - Ce)V}{Ms} \qquad (6)$$

Where (Q) (mmol g^{-1}) is the adsorbed concentration, (Ce) (mmol L^{-1}) is the equilibrium concentration, (Ci) (mmol L^{-1}) is the initial concentration, (V) (mL) is the solution volume, and (Ms) (g) is the adsorbent mass.

Adsorption edges: The effect of pH (3-8) on adsorption was tested by mixing 0.02 g of adsorbents in 50 mL of Endosulfan solution. pH was adjusted with HCl and NaOH, and the remaining concentration was measured using UV-Vis spectroscopy. An estimated removal percentage of Endosulfan was calculated by using Eq. (7).

$$\text{Removal (\%)} = \frac{Ci - Ce}{Ci} \times 100 \qquad (7)$$

Where Ci is initial concentration of endosulfan and Ce is concentration of endosulfan at equilibrium.

RESULTS AND DISCUSSION

Adsorption kinetics: The study assessed the adsorption efficiency of various inorganic and organic adsorbents for removing endosulfan from aqueous solutions. The maximum adsorption capacity was observed with natural zeolite and magnetite application among the other materials. Adsorption kinetics revealed that clay minerals and magnetite achieved maximum adsorption capacity at a low endosulfan concentration (0.01 mg L^{-1}) within 16 hours (Fig. 1). Adsorption efficiency increased slightly before reaching equilibrium at 24 hours, where the curves stabilized, indicating equilibrium. Among the inorganic adsorbents, natural zeolite exhibited the highest efficiency, exceeding that of magnetite. Magnetite has a triple positive charge and a high iron oxidation state that enhance its Lewis acid properties, promoting interactions with sulfate radicals of endosulfan (Cheng *et al*., 2021; Bulgariu *et al*., 2024). In aqueous phases, endosulfan releases sulfate radicals, allowing adsorption at active sites and forming iron chelates (Jain *et al*., 2020). Additionally, π-electrons on magnetite facilitate coordination with the carbonyl oxygen of the endosulfan radical, further enhancing its adsorption capacity (Das *et al*., 2017). These findings show the effectiveness of inorganic adsorbents, particularly clay minerals, in mitigating endosulfan in wastewater.

For feedstock and its biochar, the maximum adsorption capacity was also observed at 16 hours (Fig. 1). Toward 24 hours, adsorption efficiency remained consistent, with a minor uplift in the equilibrium curve at both low (0.01 mg L^{-1}) and high (1 mg L^{-1}) endosulfan concentrations (Figs. 1 and 2). Kinetics data further indicated that biochar exhibited a higher removal efficiency compared to its natural counterparts. The adsorption equilibrium data showed a consistent removal trend across all adsorbents, starting slow, increasing gradually, and stabilizing at equilibrium (16–24 hours). Initially, reverse adsorption dominated, shifting to forward adsorption in the mid-phase, achieving dynamic equilibrium (Qc = Kc). At this point, saturated adsorption sites prevented further adsorption. Maximum adsorption capacity correlated with the availability of vacant sites, with biochar outperforming natural materials in endosulfan removal. Relative adsorption efficiencies for the tested adsorbents were ranked as follows: natural zeolite > magnetite > kaolinite > sugarcane biochar > montmorillonite > sawdust biochar > corncob biochar > sawdust natural > sugarcane bagasse > corncob natural (Figs. 1 and 2). This ranking underscores the effectiveness of inorganic adsorbents, particularly natural zeolite and magnetite, in pollutant removal. The findings of this study are consistent with those of previous research. Saha *et al*. (2014) observed similar adsorption behavior when studying pesticide removal using rice husk ash, with adsorption times ranging from 120 to 240 minutes. This aligns with our results, where adsorption efficiency was found to increase with time before reaching equilibrium. Similarly, Boivin *et al*. (2005) reported greater desorption for hydrophilic pesticides, such as atrazine (91.1%), compared to hydrophobic ones like trifluralin (17.3%). They attributed this difference to the higher water solubility of hydrophilic pesticides and their weaker interactions with soil components, such as organic matter and clay particles. Our study also suggests that the adsorption efficiency of various adsorbents, including natural zeolite and magnetite, is influenced by the chemical properties of the target contaminant. Additionally, Yadav and Singh (2021) obtained results in line with our findings, further supporting the conclusion that adsorption efficiency is affected by both the nature of the adsorbent and the pollutant. These studies collectively reinforce the importance of understanding the interactions between adsorbents and contaminants in optimizing the removal process.

Kinetics modeling of Endosulfan: The kinetic data for the adsorption of endosulfan at a concentration of 0.01 mg L^{-1} were analyzed using the pseudo-first order, pseudo-second order, and intra-particle diffusion models. As shown in Table 1, the pseudo-second-order model provided the best fit for all organic and inorganic adsorbents, except for montmorillonite. For montmorillonite, the experimental adsorption capacity (Qe Exp) was 1.89 mg g^{-1}, while the maximum adsorption capacity (Qe max) predicted by the pseudo-first and pseudo-second-order models was 1.93 mg g^{-1} and 2.02 mg g^{-1}, respectively. The pseudo-first-order model yielded a better fit to the experimental data, with an R^2 value of 0.977, indicating a closer match between the predicted and observed adsorption capacities. The R^2 values of 0.99 and the similarity between the Qe max and Qe Exp values confirmed the strong correlation between the experimental and predicted adsorption capacities. The second-order model suggests that surface-active site availability is a limiting factor for adsorption, as noted by Singh *et al*. (2018). Chemisorption, driven by interactions with functional groups, was identified as the dominant mechanism for most adsorbents, except for montmorillonite (Fierro *et al*., 2008). Intra-particle diffusion was found to be the fastest for sawdust, corncob biochar, and montmorillonite, with Kid values of 0.3093, 0.3075, and 0.3067, respectively (Wu *et al*., 2009). Adsorption was influenced by both film and pore surface diffusion, as observed by Tran *et al*. (2017). The large BLT values (0.365–1.43 mg g^{-1}) indicated that endosulfan diffused through the aqueous layer, and stirring could reduce BLT, enhancing diffusion and

facilitating steady adsorption dominated by intra-particle processes (Fierro *et al*., 2008).

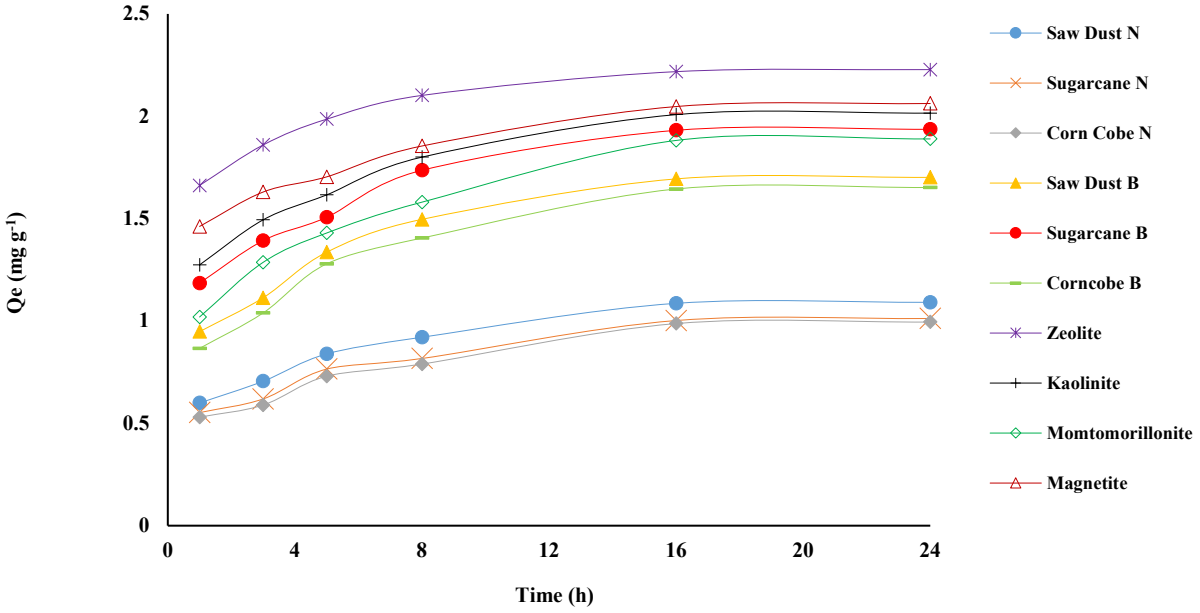

Fig. 1. Adsorption kinetics of Endosulfan onto different adsorbents at a 0.01 mg L^{-1} concentration of Endosulfan at different time intervals. On the x-axis, values show time in hours, and on the y-axis, values are showing adsorption capacity at equilibrium (Qe).

Saw Dust N; saw dust normal, sugarcane N; sugarcane normal, Corncob N; corncob normal, Saw Dust B; saw dust biochar, Sugarcane B; sugarcane biochar, Corncob B; corncob biochar.

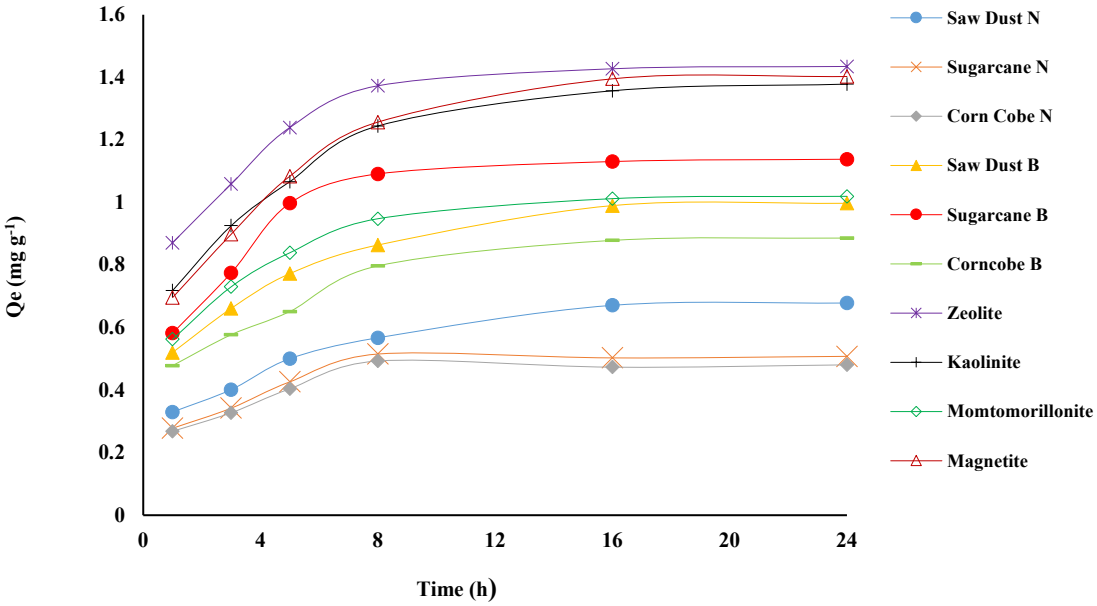

Fig. 2. Adsorption kinetics of Endosulfan onto different adsorbents at a 1 mg L^{-1} concentration of Endosulfan at different time intervals. On the x-axis, values are showing time in hours, and on the y-axis, values are showing adsorption capacity at equilibrium (Qe).

Saw Dust N; saw dust normal, sugarcane N; sugarcane normal, Corncob N; corncob normal, Saw Dust B; saw dust biochar, Sugarcane B; sugarcane biochar, Corncob B; corncob biochar.

Table 1. Pseudo-first order and Pseudo-second order model output for Endosulfan adsorption on different adsorbents at different time intervals.

Model		Pseudo-first order			Pseudo-second order		
Adsorbent	$Q_{e\ Exp}$ (mg g^{-1})	K_1 (min^{-1})	$Q_{1e\ max}$ (mg g^{-1})	R^2	K_2 (g mg^{-1} min^{-1})	$Q_{2e\ max}$ (mg g^{-1})	R^2
Natural Zeolite	2.23	0.2503	0.79	0.996	0.7264	2.28	0.999
Magnetite	2.07	0.2510	1.08	0.984	0.5086	2.13	0.998
Kaolinite	2.02	0.2425	1.15	0.966	0.3773	2.12	0.997
Montmorillonite	1.89	0.3277	1.93	0.977	0.9276	2.02	0.997
Sugarcane Bagasse Biochar	1.94	0.2556	1.16	0.961	0.3860	2.04	0.998
Sawdust Biochar	1.71	0.2148	1.01	0.962	0.3652	1.81	0.998
Corncob Biochar	1.66	0.2203	1.09	0.959	0.3260	1.77	0.997
Sawdust Natural	1.1	0.1943	0.65	0.950	0.5122	1.16	0.997
Sugarcane Bagasse	1.1	0.1943	0.65	0.950	0.5122	1.16	0.997
Corncob Natural	1	0.2155	0.74	0.961	0.4421	1.08	0.993

Note: $Q_{e\ Exp}$; experimental adsorption capacity, $Q_{1e\ max}$; maximum adsorption capacity at first order, K_1; rate constant for pseudo-first-order adsorption, K_2; rate constant for pseudo-second-order adsorption, $Q_{2e\ max}$; maximum adsorption capacity at first order, R^2; fitness of model.

Table 2. Intra-particle diffusion model output for Endosulfan at different adsorbents.

Adsorbents	K_{id} (mg [g $min^{0.5}$]$^{-1}$)	BLT (mg g^{-1})	R^2
Natural Zeolite	0.2422	1.4303	0.9945
Magnetite	0.2099	1.2535	0.9928
Kaolinite	0.2718	0.9525	0.9525
Montmorillonite	0.3067	0.7312	0.9918
Sugarcane Bagasse Biochar	0.2948	0.8803	0.9893
Sawdust Biochar	0.3093	0.6205	0.9845
Corncob Biochar	0.3075	0.5479	0.9778
Sawdust Natural	0.182	0.4114	0.9846
Sugarcane Bagasse	0.182	0.4114	0.9846
Corncob Natural	0.1512	0.3651	0.9462

Note: K_{id}; intra-particle diffusion rate constant, BLT; amount of adsorbate adsorbed at time t, R^2; fitness of model.

Isothermal adsorption of Endosulfan: The adsorption isotherm data for various adsorbents revealed that, overall, inorganic adsorbents exhibited higher removal efficiency compared to organic adsorbents, except sugarcane biochar, which showed greater adsorption capacity than montmorillonite (Fig. 3). The superior adsorption capacity of sugarcane biochar can be attributed to the presence of silicon groups on its surface, which enhance its adsorption properties. Among the inorganic adsorbents, magnetite demonstrated the highest removal efficiency, surpassing all organic adsorbents except natural zeolite. Natural zeolite, often referred to as a "chemical sieve," has a high number of exchangeable anions and cations on its surface, contributing to its adsorption capacity. Additionally, natural zeolite is particularly effective in adsorbing organic benzene-based pollutants (Zeb *et al*., 2020). The high adsorption efficiency of magnetite is primarily due to its triple positive charge, high oxidation state, and strong ability to accept electron pairs. Furthermore, magnetite's transitional iron phase, with its abundant π-electrons, facilitates coordination with the carbonyl oxygen of the endosulfan radical, enhancing its adsorption capacity.

Inorganic adsorbents exhibit high adsorption due to abundant binding sites and strong interactions, such as ionic, covalent, or coordinate covalent bonds. Endosulfan's sulfate radicals and the carbonyl group of the pollutant favor substitution reactions with clay minerals and magnetite. Clay minerals adsorb both anionic and cationic pollutants, with exchangeable ions on their surface facilitating quantitative reactions. The stability of clay particles in colloidal suspensions, influenced by surface area, charge, and cation exchange capacity, enhances their ability to retain pollutants. At 0.01 mg L^{-1} endosulfan concentration, natural zeolite outperformed magnetite by 6%, and inorganic adsorbents showed higher efficiency than organic ones (Fig. 3).

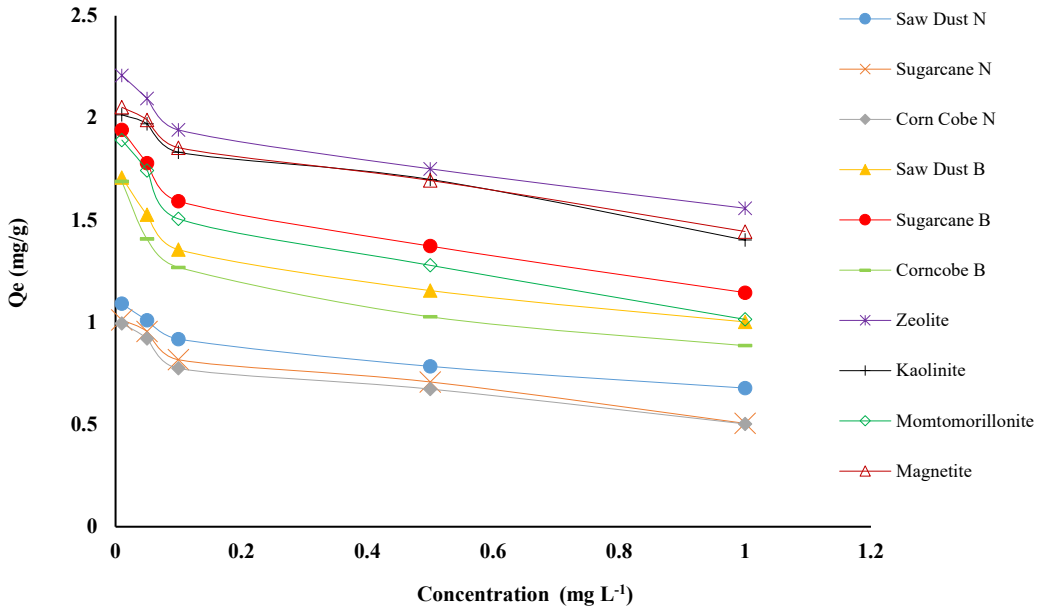

Fig. 3. Adsorption isotherm of Endosulfan at different concentrations onto different adsorbents.
Saw Dust N; saw dust normal, sugarcane N; sugarcane normal, Corncob N; corncob normal, Saw Dust B; saw dust biochar, Sugarcane B; sugarcane biochar, Corncob B; corncob biochar.

Adsorption edges: In the present study, the role of pH for the adsorption of endosulfan (0.01 and 1 mg L^{-1}) was investigated at different pH (3-8) on different organic (feedstock and their biochar) and inorganic (clay minerals and magnetite) adsorbents. The other experimental conditions, such as temperature and solid adsorbent dose, were kept constant to investigate the ionization effect by changing pH values. Different studies have shown the importance of pH in the adsorption process. Various functional groups (hydroxyl, COOH, carboxylate, etc.) can be found on the surface of adsorbents. The interaction of these functional groups varies and depends on the pH of the solution (Oh and Seo, 2019). Ionization plays a major role in controlling the adsorption process. The adsorption edge data showed that all inorganic adsorbents had higher adsorption efficiency than organic adsorbents.

The pH of the solution is directly related to some factors, as the pH has a direct influence on the value of the zero-point charge (Pzc) of the solution. For inorganic adsorbents, the relationship between pH and pHpzc (pH < pHpzc) has a higher value than for organic adsorbents and thus higher removal efficiency for endosulfan from contaminated water. The pH of the solution is directly correlated with some factors, as the pH has a direct influence on the value of the zero-point charge (Pzc) of the solution. It should be noted here that it must be a quantitative value and not a qualitative value. Once this condition (Pzc) is achieved, no reactants will move from each side in the presence of the electric field. In the case of Endosulfan, the sulfate radical attached to the carbonyl carbon of the double benzene ring is detached and thus creates a lone pair of electrons on the oxygen of the carbonyl carbon. This was the main active site for the formation of endosulfan and adsorbent chelates. If the pH < pHpzc, it means that the condition is acidic, and the pH (3) is low. So, under this condition, the adsorption was maximum for whole of the adsorption reaction (Figs. 4 and 5). At that pH, the adsorbent was positively charged and the pollutant radical was negatively charged; hence, the adsorption was maximum, and when pH > $pH_{pzc,}$ the adsorbent surface was negatively charged, and hence the adsorption was low at a high pH level.

Clay minerals have different ionizing behavior due to the presence of inner and outer-sphere complexation mechanisms towards a variety of pollutants. Also, H-bonding between clay and pollutant legend due to the presence of water in the shape of ions is most favorable factor for adsorption. Moreover, the surface OH-group of clay minerals interacts with π electrons of the aromatic pollutant ring of endosulfan. Also, the redox reactions on the surface of clay minerals and magnetite favor the adsorption mechanism. Moreover, in case of clay minerals, magnetite had a high value of reaction quotient (Q_c), and the adsorption reaction was more in the forward direction as compared to the reverse direction. However, in the case of organic adsorbents, the relation between reaction quotient (Q_c) and equilibrium constant (K_c) was not as mature as in the case of inorganic one. In the case of clay minerals, it refers to the replacement of compensatory cations inside a solid phase. It is quite possible that specific chemical

bonds are formed when endosulfan radicals are adsorbed onto clay minerals. However, there is one type of chemical bonding that is very important for contaminants and clay mineral systems, and that is coordinative bonding with metal cations. Adsorption order in case of relative efficiency among different inorganic and organic adsorbents at different pH levels was as natural. zeolite > magnetite > kaolinite > montmorillonite > sugarcane biochar > sawdust biochar > corncob biochar > sawdust natural > sugarcane bagasse > corncob natural. In the case of isothermal sugarcane biochar had greater efficiency as compared to montmorillonite but at pH experiment the result was different.

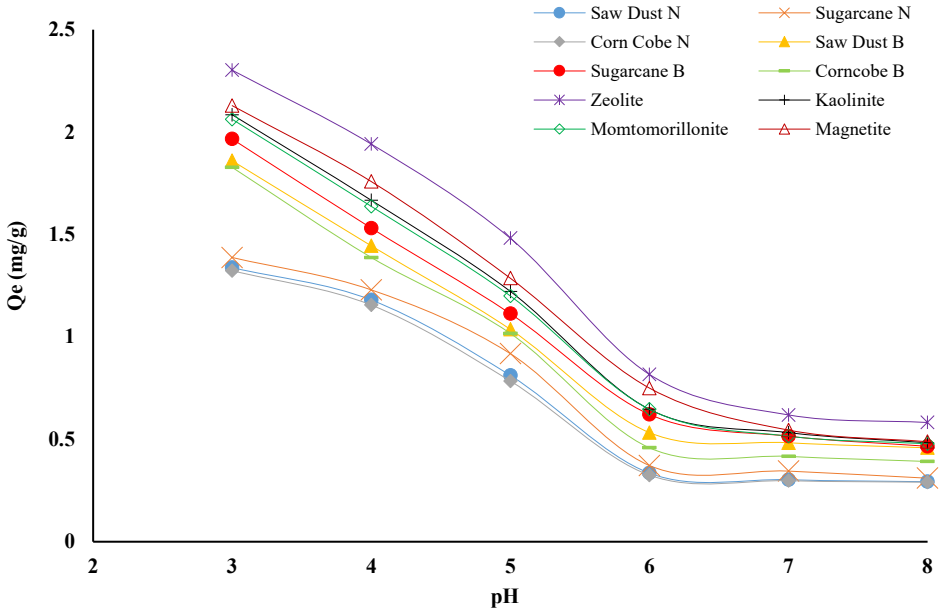

Fig. 4. Adsorption edges of Endosulfan (0.1 mg L^{-1}) onto different adsorbents at different pH levels of solution medium.

Saw Dust N; saw dust normal, sugarcane N; sugarcane normal, Corncob N; corncob normal, Saw Dust B; saw dust biochar, Sugarcane B; sugarcane biochar, Corncob B; corncob biochar.

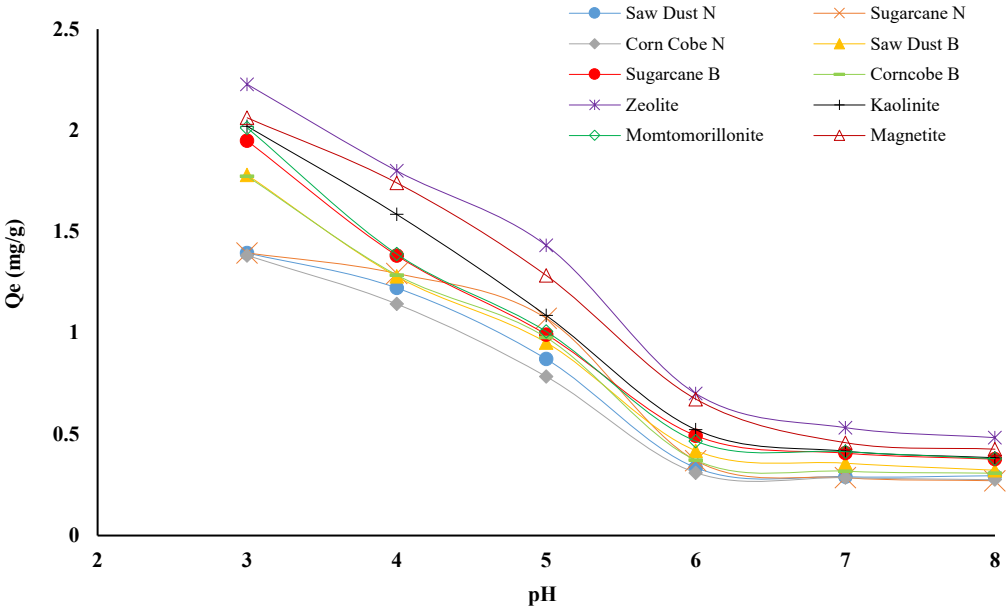

Fig. 5. Adsorption edges of Endosulfan (1 mg L^{-1}) onto different adsorbents at different pH levels of solution medium.

Saw Dust N; saw dust normal, sugarcane N; sugarcane normal, Corncob N; corncob normal, Saw Dust B; saw dust biochar, Sugarcane B; sugarcane biochar, Corncob B; corncob biochar.

Scanning Electron Microscopy (SEM) of inorganic Adsorbents for pre and post adsorption experiment: SEM analysis was done based on pre- and post-batch adsorption experiments for different inorganic adsorbents, including natural zeolite, montmorillonite, kaolinite, and magnetite. The SEM analysis showed that the natural zeolite was highly crystalline, which was supported by the XRD results of our study. Overall, the sample had a flake-like crystal configuration with a smaller number of impurities. Pre- and post-batch adsorption SEM analysis of natural zeolite (Fig. 6) expressed the clear changes in edge morphology and proved the endosulfan adsorption during the batch adsorption experiment. The SEM images of montmorillonite showed (Fig. 7) the surface morphology of montmorillonite, which was loose and porous, while after the adsorption experiment, the surface of montmorillonite became smooth and neat.

SEM analysis of kaolinite (Fig. 8) provides a comparison of the surface morphology before and after adsorption study. Pre adsorption sample depicted the morphological surface of raw kaolin particles, where hexagonal flakes were layered on top of one another with a constant distribution of micro-pores. The SEM image after adsorption experiment demonstrated that the surface structure of the kaolinite was transformed to a relatively flat surface with low porosity as a result of Endosulfan deposition. SEM images of magnetite have been shown in Fig. 9. It was discovered that the majority of them were cubic in nature and irregular in shape. Also, the particles were agglomerated to produce a foam in the form of a cluster of particles. Previous research has found a similar phenomenon. This also demonstrated the creation of ferrous nanoparticles having a cubic shape.

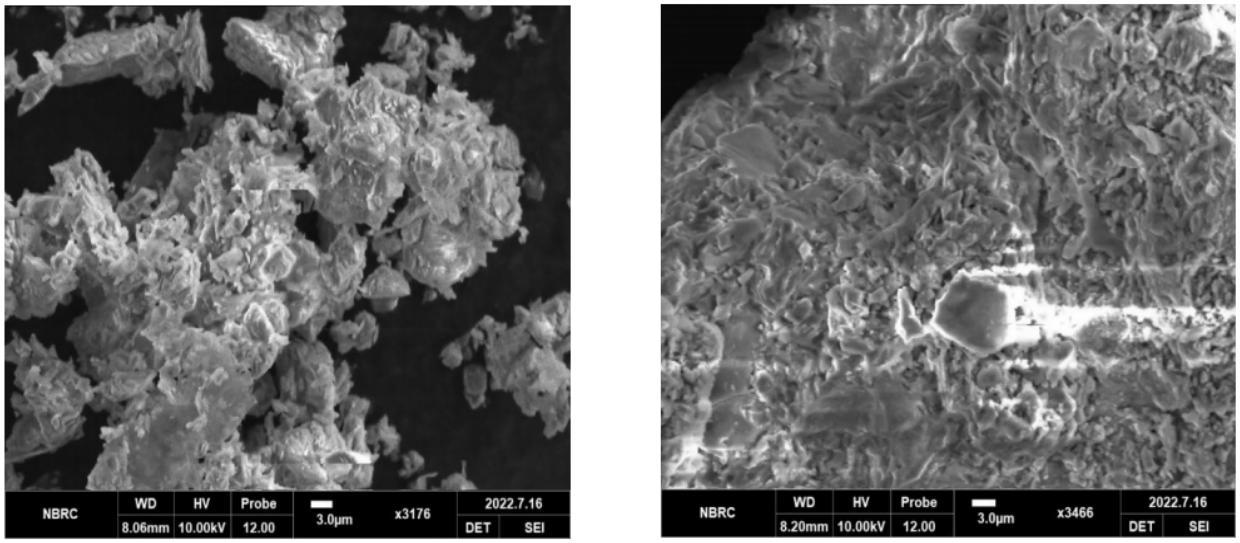

Fig. 6. SEM images of natural zeolite for pre (left) and Post (right) batch adsorption experiment.

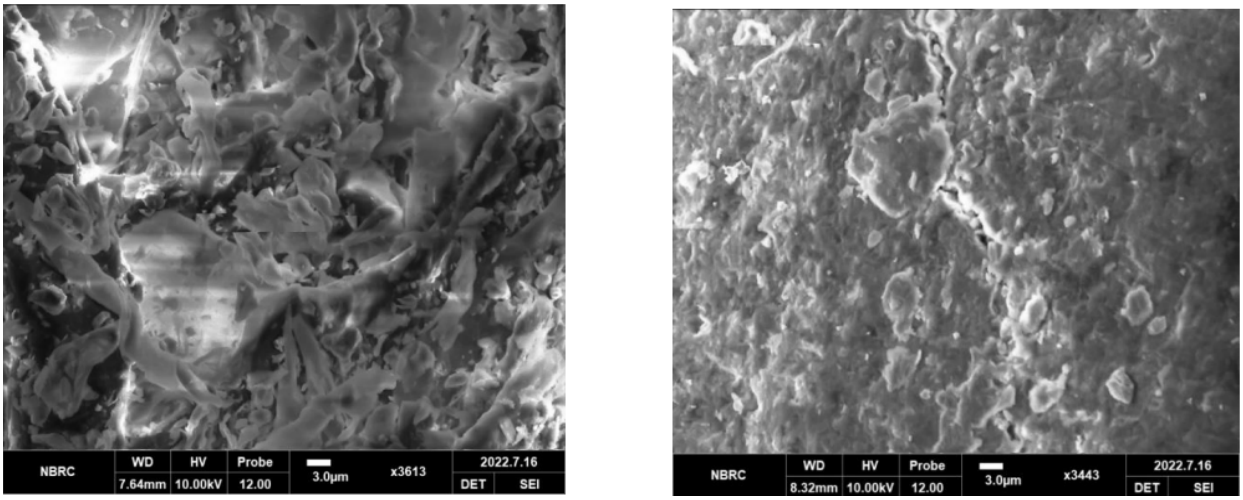

Fig. 7. SEM images of montmorrilonite for pre (left) and Post (right) batch adsorption experiment.

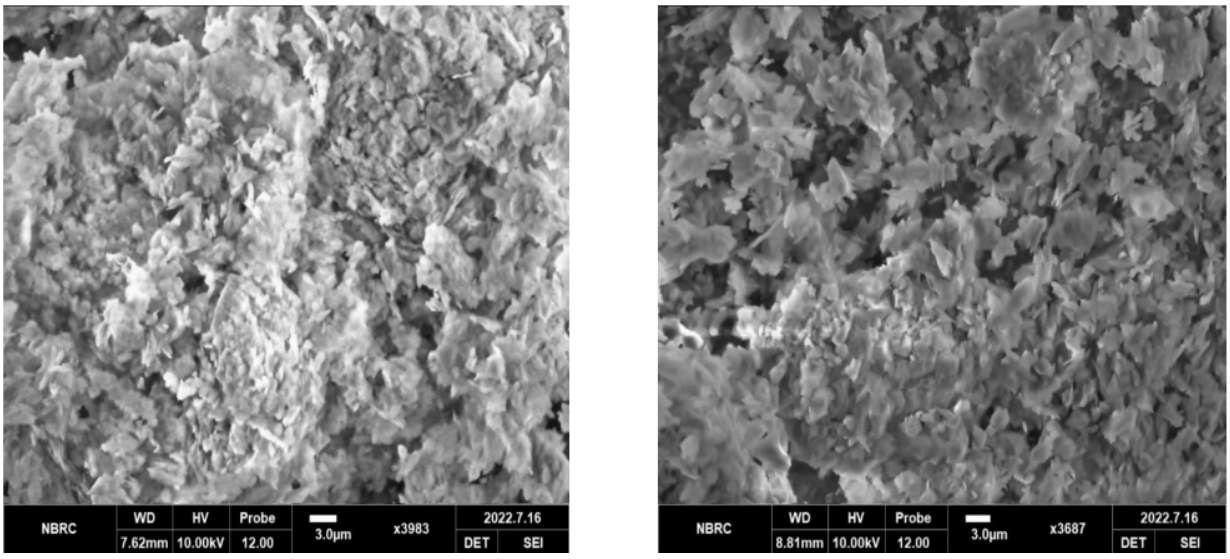

Fig. 8. SEM images of kaolinite for pre (left) and Post (right) batch adsorption experiment.

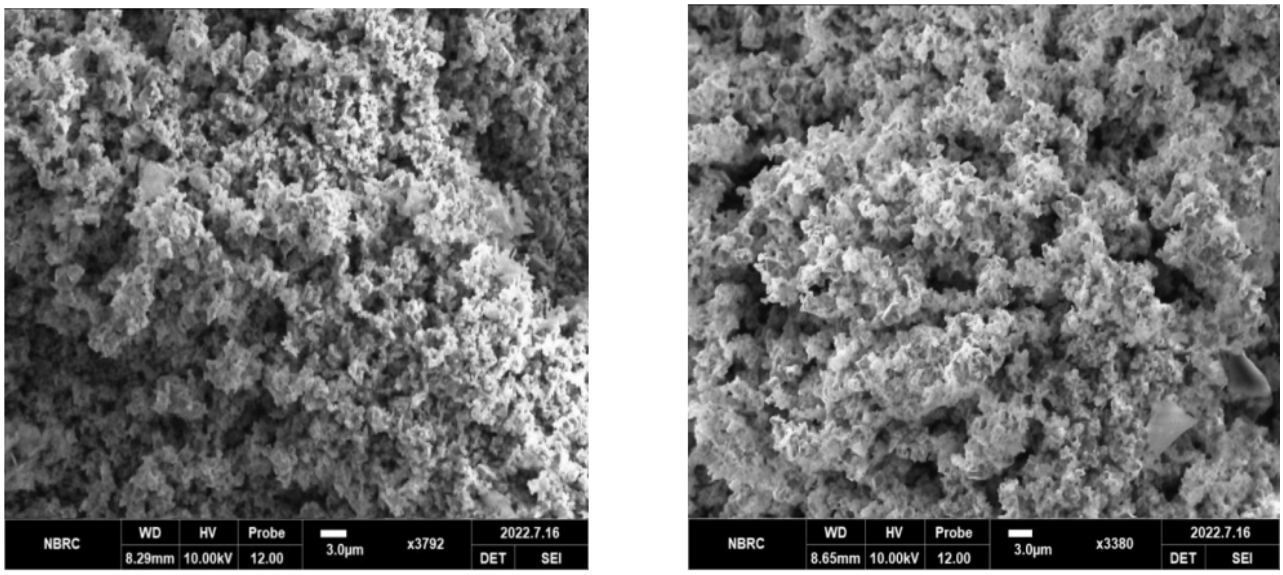

Fig. 9. SEM images of magnetite for pre (left) and Post (right) batch adsorption experiment.

Conclusions: A batch adsorption experiment was conducted to evaluate the adsorption of endosulfan onto various organic and inorganic adsorbents. Among inorganic adsorbents, natural zeolite exhibited the highest adsorption capacity, while biochar showed superior performance among organic adsorbents. The results indicated that inorganic adsorbents had a higher affinity for chelate formation with endosulfan and reached adsorption saturation more quickly than organic adsorbents.

Kinetic modeling revealed that the pseudo-second-order model best described the adsorption process, confirming chemisorption. The intra-particle diffusion model suggested that endosulfan initially faced resistance in diffusing into the inner surfaces of the adsorbents, leading to a multilayer adsorption mechanism followed by monolayer adsorption.

Characterization of adsorbents before and after adsorption further validated these findings. FTIR and XRD analyses confirmed the presence of functional groups responsible for adsorption, while SEM analysis evidenced the deposition of endosulfan crystals and alterations in surface morphology.

Additionally, the study highlighted the critical role of pH (3–8) in adsorption efficiency. Inorganic adsorbents, particularly clay minerals and magnetite, demonstrated superior performance due to their abundant functional groups, high ion exchange capacity, and stability in colloidal suspensions. The findings emphasize the significance of ionization and functional group

interactions in governing adsorption behavior, offering valuable insights for optimizing adsorbent selection in endosulfan-contaminated water remediation.

Acknowledgement: We, the authors are very thankful to Higher Education Commission (HEC), Islamabad for providing funds (PIN # 48BMS17) to conduct this research. The authors acknowledge the support and research facilities from the University of Agriculture, Faisalabad. Further, we acknowledge the research support from Nicole Jaffrezic-Renault (Emeritus Research Director in Centre National de la Recherche Scientifique (CNRS)).

Conflict of Interest: Authors declare no conflict of interest.

Data Availability: Available on request to corresponding author.

Author Contribution: Muhammad Aamer Hussain has collected the material, performed the research, and prepared and analyzed the samples. Ghulam Murtaza has supervised the whole research. Muhammad Zia-ur-Rehman has provided his expertise in statistical data analysis and preparation of figures. Muhammad Shahid has helped in interpreting the SEM images and writing and critically reviewing the manuscript. Analytical work was carried out at Eindhoven University of Technology, Eindhoven, Netherlands under the supervision of Sofia Calero.

Funding Declaration: Higher Education Commission (HEC), Islamabad, Pakistan provided funds under International Research Support Initiative Program (IRSIP) (PIN # 48BMS17) to conduct research at Eindhoven University of Technology, Eindhoven, Netherlands.

Animal Research: Not applicable.

Consent to Publish: All the authors are willing and have no conflict in publishing the article in this journal.

REFERENCES

Abbas, M., S. Abbas, N. Hussain, M.T. Javeed, A. Ghaffar, M. Nadeem, M. Khaliq, S. Ullah, Z. Parveen, K.A. Khan and H.A. Ghramh (2024). Assessment of residues from common pesticides and associated risks in Pakistan. Environ. Monit. Assess. 196: 1061. https://doi.org/10.1007/s10661-024-13220-x

Ashraf, A., I. Bibi, N.K. Niazi, Y.S. Ok, G. Murtaza, M. Shahid, A. Kunhikrishnan, D. Li and T. Mahmood (2017). Chromium(VI) sorption efficiency of acid-activated banana peel over organo-montmorillonite in aqueous solutions. Int. J. Phytoremediation. 19: 605–613. https://doi.org/10.1080/15226514.2016.1256372

Aslan, Ş. and A. Türkman (2004). Simultaneous biological removal of endosulfan (α+β) and nitrates from drinking waters using wheat straw as substrate. Environ. Int. 30: 449–455. https://doi.org/10.1016/s0160-4120(03)00092-8

Aziz, K., R. Mamouni, S. Kaya and F. Aziz (2024). Low-cost materials as vehicles for pesticides in aquatic media: a review of the current status of different biosorbents employed, optimization by RSM approach. Environ. Sci. Pollut. Res. 31: 39907–39944. https://doi.org/10.1007/s11356-023-27640-8

Bhanot, K. and A. Pant (2025). Toxicological effect, bioaccumulative potential, and risk assessment of endosulfan. In Hazardous Chemicals (pp. 137-155). Academic Press. https://doi.org/10.1016/b978-0-323-95235-4.00053-0

Boivin, A., R. Cherrier and M. Schiavon (2005). A comparison of five pesticides adsorption and desorption processes in thirteen contrasting field soils. Chemosphere. 61: 668–676. https://doi.org/10.1016/j.chemosphere.2005.03.024

Bulgariu, L., M. Gavrilescu and D.I. Fertu (2024). Sustainable use of some natural materials and waste for the decontamination of environmental components polluted with heavy metals. Environ. Eng. Manag. J. 23: 1543–1569. https://doi.org/10.30638/eemj.2024.126

Cheng, R., M. Kang, L. Shi, J. Wang, X. Zheng and J. Wang (2021). Fe-based nanomaterials for removing the environmental endocrine disrupting chemicals in water: A Review. Environ. Nano. 5: 261-292. https://doi.org/10.1007/978-3-030-73010-9_7

Cooney, E., G. Stevens, N. Booker and D. Shallcross (1999). Ammonia removal from wastewaters using natural Australian zeolite. II. Pilot-scale study using continuous packed column process. Sep. Sci. Technol. 34: 2741–2760. https://doi.org/10.1081/ss-100100802

Das, R., C.D. Vecitis, A. Schulze, B. Cao, A.F. Ismail, X. Lu, J. Chen and S. Ramakrishna (2017). Recent advances in nanomaterials for water protection and monitoring. Chem. Soc. Rev. 46: 6946–7020. https://doi.org/10.1039/c6cs00921b

Dilna, C., G.K. Prasanth and S.R. Kanade (2018). Molecular interaction studies of endosulfan with the cholinergic pathway targets – An insilico approach. Comput. Toxicol. 5: 1–7. https://doi.org/10.1016/j.comtox.2017.11.002

Durán, E., S. Bueno, M.C. Hermosín, L. Cox and B. Gámiz (2019). Optimizing a low added value

bentonite as adsorbent material to remove pesticides from water. Sci. Total Environ. 672: 743–751. https://doi.org/10.1016/j.scitotenv.2019.04.014

Fantke, P. and O. Jolliet (2016). Life cycle human health impacts of 875 pesticides. Int. J. Life Cycle Assess. 21: 722–733. https://doi.org/10.1007/s11367-015-0910-y

Fierro, V., V. Torné-Fernández, D. Montané and A. Celzard (2008). Adsorption of phenol onto activated carbons having different textural and surface properties. Microporous Mesoporous Mater. 111: 276–284. https://doi.org/10.1016/j.micromeso.2007.08.002

Fraiha, O., N. Hadoudi, N. Zaki, A. Salhi, H. Amhamdi, E.H. Akichouh, F. Mourabit and M. Ahari (2024). Comprehensive review on the adsorption of pharmaceutical products from wastewater by clay materials. Desalin. Water Treat. 317: 100114. https://doi.org/10.1016/j.dwt.2024.100114

Jacobson, M.H., Y. Wu, M. Liu, K. Kannan, A.J. Li, M. Robinson, B.A. Warady, S. Furth, H. Trachtman and L. Trasande (2021). Organophosphate pesticides and progression of chronic kidney disease among children: A prospective cohort study. Environ. Int. 155: 106597. https://doi.org/10.1016/j.envint.2021.106597

Jain, M., A. Mudhoo, D.L. Ramasamy, M. Najafi, M. Usman, R. Zhu, G. Kumar, S. Shobana, V.K. Garg and M. Sillanpää (2020). Adsorption, degradation, and mineralization of emerging pollutants (pharmaceuticals and agrochemicals) by nanostructures: a comprehensive review. Environ. Sci. Pollut. Res. 27: 34862–34905. https://doi.org/10.1007/s11356-020-09635-x

Juela, D.M. (2022). Promising adsorptive materials derived from agricultural and industrial wastes for antibiotic removal: a comprehensive review. Sep. Purif. Technol. 284: 120286. https://doi.org/10.1016/j.seppur.2021.120286

Karami-Mohajeri, S. and M. Abdollahi (2011). Toxic influence of organophosphate, carbamate, and organochlorine pesticides on cellular metabolism of lipids, proteins, and carbohydrates: a systematic review. Hum. Exp. Toxicol. 30(9): 1119-1140. https://doi.org/10.1177/0960327110388959

Karim, A.A., M. Kumar, S. Mohapatra and S.K. Singh (2019). Nutrient rich biomass and effluent sludge wastes co-utilization for production of biochar fertilizer through different thermal treatments. J. Clean. Prod. 228: 570–579. https://doi.org/10.1016/j.jclepro.2019.04.330

Khandamov, D.A., T.A. Kurniawan, A.S. Bekmirzayev, F. Batool, D. Khandamova, S. Nurullayev, S. Kholikova, Z. Babakhanova and M.M. Hayet Khan (2025). Enhanced adsorption of Fe(II) from synthetic wastewater using modified bentonite: Isotherms, kinetics, thermodynamics, and adsorption mechanisms. Microporous Mesoporous Mater. 384: 113451. https://doi.org/10.1016/j.micromeso.2024.113451

Khoo, R.Z., W.S. Chow and H. Ismail (2018). Sugarcane bagasse fiber and its cellulose nanocrystals for polymer reinforcement and heavy metal adsorbent: a review. Cellulose. 25: 4303–4330. https://doi.org/10.1007/s10570-018-1879-z

Li, Z. and A. Jennings (2017). Worldwide regulations of standard values of pesticides for human health risk control: a review. Int. J. Environ. Res. Public Health. 14: 826. https://doi.org/10.3390/ijerph14070826

Li, Z., J. Qiu, X. Xu, R. Wan, M. Yao, H. Wang, Z. Zhou and J. Xu (2025). Solar driven kaolin-based hydrogels for efficient interfacial evaporation and heavy metal ion adsorption from wastewater. Sep. Purif. Technol. 354: 129243. https://doi.org/10.1016/j.seppur.2024.129243

Liu, G., L. Li, D. Xu, X. Huang, X. Xu, S. Zheng, Y. Zhang and H. Lin (2017). Metal–organic framework preparation using magnetic graphene oxide–β-cyclodextrin for neonicotinoid pesticide adsorption and removal. Carbohydr. Polym. 175: 584–591. https://doi.org/10.1016/j.carbpol.2017.06.074

Liu, G., Z. Dai, X. Liu, R.A. Dahlgren and J. Xu (2022). Modification of agricultural wastes to improve sorption capacities for pollutant removal from water : a review. Carbon Res. 1: 1-24. https://doi.org/10.1007/s44246-022-00025-1

Liu, H., J. Long, K. Zhang, M. Li, D. Zhao, D. Song and W. Zhang (2024). Agricultural biomass/waste-based materials could be a potential adsorption-type remediation contributor to environmental pollution induced by pesticides-A critical review. Sci. Total Environ. 946: 174180. https://doi.org/10.1016/j.scitotenv.2024.174180

Liu, Y., L. Lonappan, S.K. Brar and S. Yang (2018). Impact of biochar amendment in agricultural soils on the sorption, desorption, and degradation of pesticides: a review. Sci. Total Environ. 645: 60–70. https://doi.org/10.1016/j.scitotenv.2018.07.099

Mandal, A., N. Singh and T.J. Purakayastha (2017). Characterization of pesticide sorption behaviour of slow pyrolysis biochars as low cost adsorbent for atrazine and imidacloprid removal. Sci. Total

Environ. 577: 376–385. https://doi.org/10.1016/j.scitotenv.2016.10.204

Martínez-Burgos, W.J., L. Porto de Souza Vandenberghe, A.F. Murawski de Mello, J.C. de Carvalho, K.K. Valladares-Diestra, M.C. Manzoki, T. Scapini, R. Pozzan, R.K. Liew, V. Thomaz-Soccol and C.R. Soccol (2024). Bioremediation strategies against pesticides: An overview of current knowledge and innovations. Chemosphere 364: 142867. https://doi.org/10.1016/j.chemosphere.2024.142867

Mokhtar, A., B. Asli, S. Abdelkrim, M. Hachemaoui, B. Boukoussa, M. Sassi, G. Viscusi and M. Abboud (2024). Polymer/Clay nanocomposites as advanced adsorbents for textile wastewater treatment. Minerals. 14: 1216. https://doi.org/10.3390/min14121216

Mubarak, A.A., R.A. Ilyas, A.H. Nordin, N. Ngadi and M.F.M. Alkbir (2024). Recent developments in sugarcane bagasse fibre-based adsorbent and their potential industrial applications: a review. Int. J. Biol. Macromol. 277: 134165. https://doi.org/10.1016/j.ijbiomac.2024.134165

Obsa, A.L., N.T. Shibeshi, E. Mulugeta and G.A. Workeneh (2024). Bentonite/amino-functionalized cellulose composite as effective adsorbent for removal of lead: kinetic and isotherm studies. Results Eng. 21: 101756. https://doi.org/10.1016/j.rineng.2024.101756

Ogura, A.P., J.Z. Lima, J.P. Marques, L. Massaro Sousa, V.G.S. Rodrigues and E.L.G. Espíndola (2021). A review of pesticides sorption in biochar from maize, rice, and wheat residues: current status and challenges for soil application. J. Environ. Manage. 300: 113753. https://doi.org/10.1016/j.jenvman.2021.113753

Oh, S.Y. and Y.D. Seo (2019). Factors affecting the sorption of halogenated phenols onto polymer/biomass-derived biochar: Effects of pH, hydrophobicity, and deprotonation. J. Environ. Manage. 232: 145-152. https://doi.org/10.1016/j.jenvman.2018.11.064

Saha, A., V.T. Gajbhiye, S. Gupta, R. Kumar and R.K. Ghosh (2014). Simultaneous removal of pesticides from water by rice husk ash: batch and column studies. Water Environ. Res. 86: 2176–2185. https://doi.org/10.2175/106143014x14062131178358

Saleh, I.A., N. Zouari and M.A. Al-Ghouti (2020). Removal of pesticides from water and wastewater: Chemical, physical and biological treatment approaches. Environ. Technol. Innov. 19: 101026. https://doi.org/10.1016/j.eti.2020.101026

Sam, S., D. Masekela, S.P. Malinga and N. Mabuba (2025). Enhanced heavy metal piezocatalytic adsorption and antibacterial activity using kaolin-modified PVDF nanofiber mats for water treatment. J. Water Process Eng. 70: 106803. https://doi.org/10.1016/j.jwpe.2024.106803

Shakoor, M.B., N.K. Niazi, I. Bibi, G. Murtaza, A. Kunhikrishnan, B. Seshadri, M. Shahid, S. Ali, N.S. Bolan, Y.S. Ok, M. Abid and F. Ali (2016). Remediation of arsenic-contaminated water using agricultural wastes as biosorbents. Crit. Rev. Environ. Sci. Technol. 46: 467–499. https://doi.org/10.1080/10643389.2015.1109910

Singh, S., N. Parveen and H. Gupta (2018). Adsorptive decontamination of rhodamine-B from water using banana peel powder: a biosorbent. Environ. Technol. Innov. 12: 189–195. https://doi.org/10.1016/j.eti.2018.09.001

Tahervand, S. and M. Jalali (2017). Sorption and desorption of potentially toxic metals (Cd, Cu, Ni and Zn) by soil amended with bentonite, calcite and zeolite as a function of pH. J. Geochemical Explor. 181: 148–159. https://doi.org/10.1016/j.gexplo.2017.07.005

Tran, H.N., S.J. You, A.H. Bandegharaei and H.P. Chao (2017). Mistakes and inconsistencies regarding adsorption of contaminants from aqueous solutions: a critical review. Water Res. 120: 88–116. https://doi.org/10.1016/j.watres.2017.04.014

Wang, P., X. Shen, S. Qiu, L. Zhang, Y. Ma and J. Liang (2024). Clay-based materials for heavy metals adsorption: mechanisms, advancements, and future prospects in environmental remediation. Crystals. 14: 1046. https://doi.org/10.3390/cryst14121046

Wu, F.C., R.L. Tseng and R.S. Juang (2001). Kinetic modeling of liquid-phase adsorption of reactive dyes and metal ions on chitosan. Water Res. 35: 613–618. https://doi.org/10.1016/s0043-1354(00)00307-9

Wu, F.C., R.L. Tseng and R.S. Juang (2009). Initial behavior of intraparticle diffusion model used in the description of adsorption kinetics. Chem. Eng. J. 153: 1–8. https://doi.org/10.1016/j.cej.2009.04.042

Yadav, S. and N. Singh (2021). Increased sorption of atrazine and fipronil in the sugarcane trash ash–mixed soils of Northern India. J. Soil Sci. Plant Nutr. 21: 1263–1276. https://doi.org/10.1007/s42729-021-00438-8

Zeb, M.A., G. Murtaza, M.A. Hussain, K.T. Kubra, R. Muvhiiwa, L.A. De Kock and F. Hassard (2020). A comprehensive adsorption study of 1-Hydroxy-2-Naphthoic acid using cost effective engineered materials. Environ. Technol. Innov.

19: 100881. https://doi.org/10.1016/j.eti.2020.100881

Zhao, X., M. Yang, Y. Shi, L. Sun, H. Zheng, M. Wu, G. Gao, T. Ma and G. Li (2024). Multifunctional bacterial cellulose-bentonite@polyethylenimine composite membranes for enhanced water treatment: sustainable dyes and metal ions adsorption and antibacterial properties. J. Hazard. Mater. 477: 135267. https://doi.org/10.1016/j.jhazmat.2024.135267

Zhou, C. and Y. Wang (2020). Recent progress in the conversion of biomass wastes into functional materials for value-added applications. Sci. Technol. Adv. Mater. 21: 787–804. https://doi.org/10.1080/14686996.2020.1848213

Supplementary data

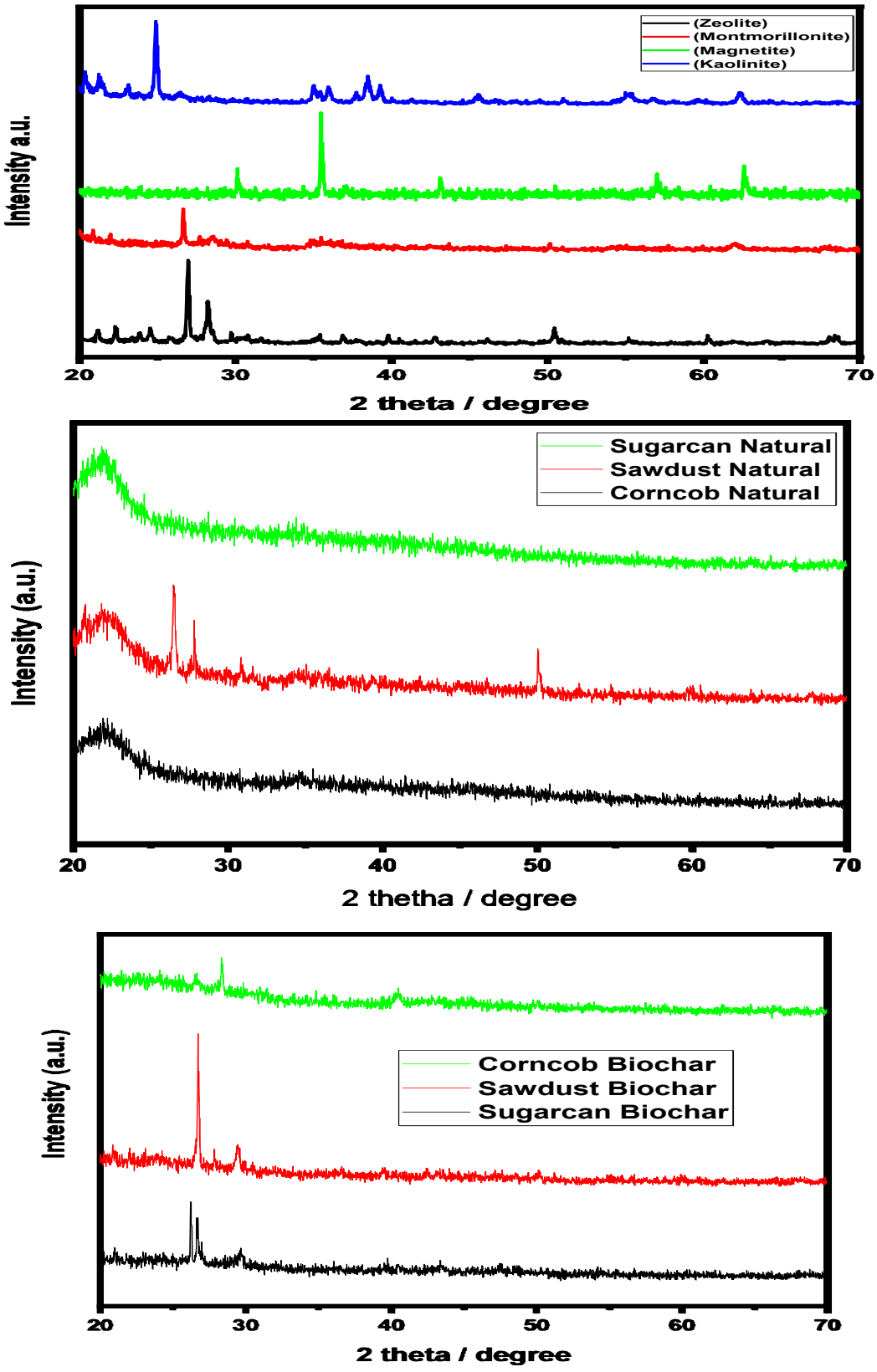

Supplementary Figure 1. X-ray diffraction of adsorbents.

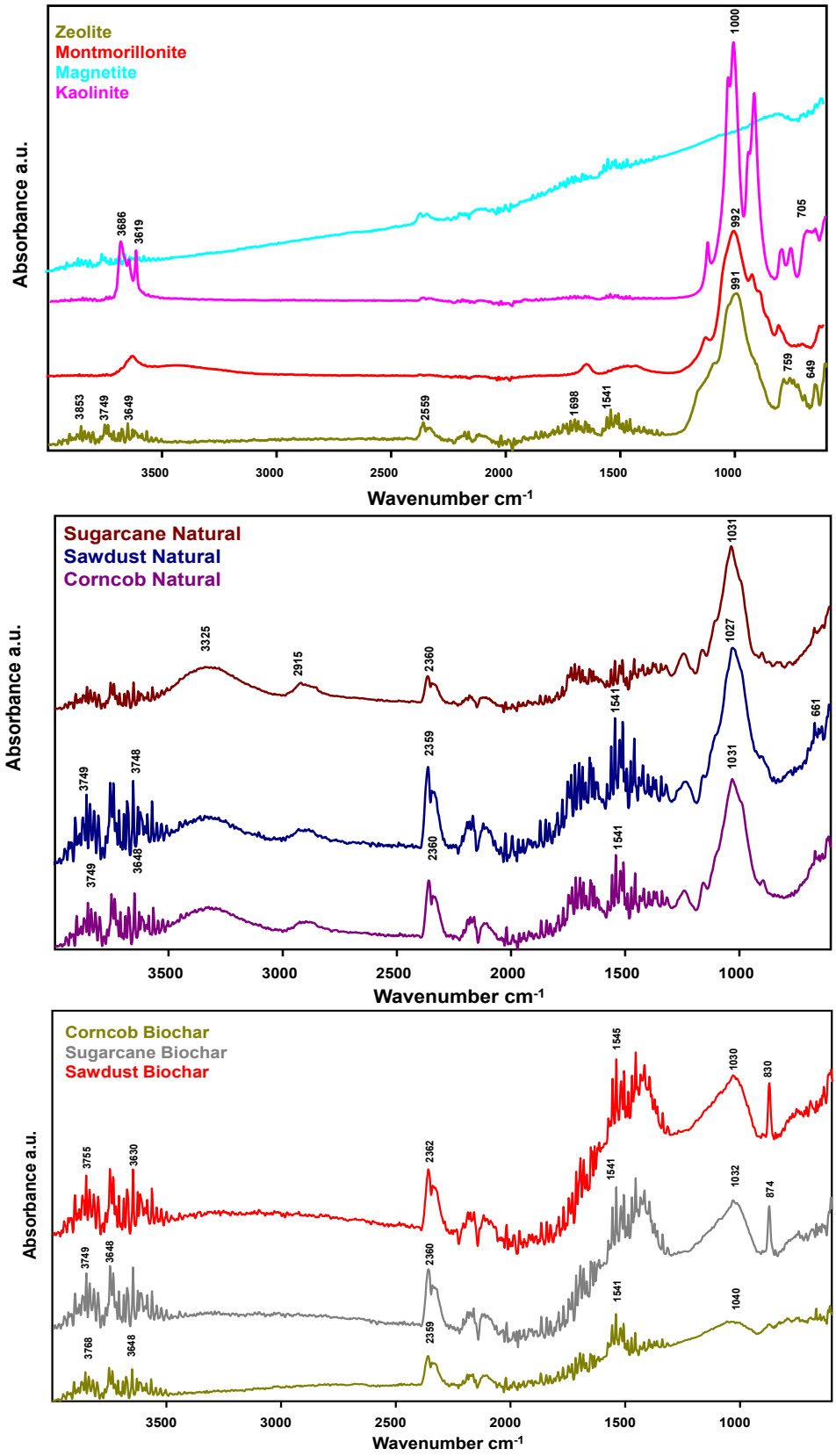

Supplementary Figure 1: FTIR analysis of adsorbents.